NACA RM L53A29

NACA

RESEARCH MEMORANDUM

LOW-SPEED LATERAL CONTROL CHARACTERISTICS OF AN UNSWEPT WING WITH HEXAGONAL AIRFOIL SECTIONS AND ASPECT RATIO 4.0 AT A REYNOLDS NUMBER OF 6.2×10^6

By William M. Hadaway

Langley Aeronautical Laboratory
Langley Field, Va.

NATIONAL ADVISORY COMMITTEE
FOR AERONAUTICS

WASHINGTON
March 20, 1953

NATIONAL ADVISORY COMMITTEE FOR AERONAUTICS

RESEARCH MEMORANDUM

LOW-SPEED LATERAL CONTROL CHARACTERISTICS OF AN UNSWEPT WING WITH HEXAGONAL AIRFOIL SECTIONS AND ASPECT RATIO 4.0 AT A REYNOLDS NUMBER OF 6.2×10^6

By William M. Hadaway

SUMMARY

A lateral-control investigation has been made in the Langley 19-foot pressure tunnel of an unswept wing having 6-percent-thick hexagonal airfoil sections, aspect ratio 4.0, and taper ratio 0.625. The wing was mounted on a circular fuselage with a fineness ratio of 10 to 1. Characteristics of both a 0.40 semispan outboard aileron and a 0.79 semispan aileron were investigated at a Reynolds number of 6.2×10^6. The effects of 0.79 semispan leading-edge flaps and 0.39 semispan trailing-edge flaps were also determined. The data include aileron normal-force, hinge-moment, and aileron balance-chamber-pressure measurements as well as force measurements by the standard six-component balance system. A theoretical aileron effectiveness value C_{l_δ} of 0.00132 compared with an experimental value of 0.00150 for the plain wing equipped with the 0.40 semispan aileron. Comparisons of the rates of change of the hinge moment with aileron deflection and angle of attack as well as C_{l_δ} of the unswept wing with those of an unswept wing of aspect ratio 2.5 having the same wing area, taper ratio, and airfoil section are also presented herein.

INTRODUCTION

As part of the study of the low-speed characteristics of wings suitable for supersonic speeds, a lateral-control investigation has been made of an unswept, modified double wedge wing of aspect ratio 4.0 in the Langley 19-foot pressure tunnel at high Reynolds numbers and low Mach numbers. Lateral-control investigations have been conducted previously for wings of similar plan form and airfoil section (NACA investigations conducted at the Ames Laboratory by Ben H. Johnson, Jr., and Fred A. Demele and by Noel K. Delany and Nora-Lee F. Hayter and at the Langley Laboratory by James E. Fitzpatrick and Robert L. Woods); however, there is a scarcity of data pertaining to aileron hinge moments, aileron normal

forces, and aileron balance-chamber pressures. This paper presents force measurements as well as aileron hinge moments, normal forces, and balance-chamber pressures. The tests included measurements of both a 0.79 semispan and an outboard 0.40 semispan aileron. The effects of leading-edge droop and part-span trailing-edge flaps on the outboard aileron effectiveness were also investigated. All tests were made with a cylindrical fuselage attached to the wing. No analysis is presented herein.

SYMBOLS AND COEFFICIENTS

The data are referred to wind axes with the origin at 25 percent of the mean aerodynamic chord projected to the plane of symmetry. Symbols and coefficients are defined as follows:

S	wing area
A	aspect ratio
λ	taper ratio
δ_n	deflection of nose flap, deg
δ_f	deflection of trailing-edge flap, deg
δ_a	deflection of aileron, deg (positive when trailing edge is down)
C_L	lift coefficient, Lift/qS
C_m	pitching-moment coefficient, Pitching moment/$qS\bar{c}$
C_n	yawing-moment coefficient, Yawing moment/qSb
C_{h_a}	aileron hinge-moment coefficient, Hinge moment/$2M_aq$
C_l	rolling-moment coefficient, Rolling moment/qSb
P_R	resultant pressure coefficient in aileron balance chamber corrected to complete sealed condition, $\left(\frac{\text{Pressure below seal - pressure above seal}}{Kq}\right)_{\text{average}}$

$$K = \left(\frac{\text{Pressure difference across seal}}{\text{Pressure difference across vents}}\right)_{\text{average}}$$

[redacted]

q	dynamic pressure, $\rho V^2/2$, lb/sq ft
$\bar{c}$	mean aerodynamic chord, $\frac{2}{S}\int_0^{b/2} c^2 dy$
b	wing span, ft
b_a	aileron span, ft
M_a	moment area of aileron behind hinge line, taken about hinge axis, $\frac{1}{2}\int_0^{b_a} {c_a}^2 dy$, cu ft
c_a	aileron chord behind and perpendicular to aileron hinge line, ft
V	free-stream velocity, ft/sec
ρ	density of air, slugs/cu ft
c	local wing chord, ft
α	angle of attack of wing root chord, deg
C_{h_α}	rate of change of aileron hinge-moment coefficient with angle of attack at $\delta_a = 0^\circ$
C_{h_δ}	rate of change of aileron hinge-moment coefficient with aileron deflection at $\delta_a = 0^\circ$
P_{R_δ}	rate of change of pressure coefficient with aileron deflection at $\delta_a = 0^\circ$
P_{R_α}	rate of change of pressure coefficient with angle of attack at $\delta_a = 0^\circ$
C_{l_δ}	rate of change of rolling-moment coefficient with aileron deflection at $\delta_a = 0^\circ$
C_{N_a}	aileron normal-force coefficient, Normal force/qS_a
S_a	aileron area behind hinge line, sq ft
R	Reynolds number, $\rho V\bar{c}/\mu$
μ	coefficient of viscosity, slugs/ft sec

[redacted]

MODEL AND TEST APPARATUS

Details of the wing model, fuselage, and aileron are presented in figure 1. The 6-percent-thick solid-steel wing had an aspect ratio of 4.0, a taper ratio of 0.625, and a sweep angle of 0° at the 50-percent chord line and had neither dihedral nor twist. The symmetrical hexagonal airfoil section had 11.42° leading- and trailing-edge angles and the upper and lower surfaces of each wing section were parallel between the 0.30 chord line and the 0.70 chord line. The wing was equipped with rounded tips. The fuselage was of circular cross section and had a fineness ratio of 10 to 1. The wing-fuselage combination was used throughout this investigation and the wing was mounted on the fuselage longitudinal center line at 0° incidence. No fillets were used at the wing-fuselage juncture.

The leading edge of the wing could be drooped from 0.16b/2 to 0.95b/2. The plain aileron was a constant 25 percent of the wing chord and extended from 0.16b/2 to 0.95b/2 on the left wing. The aileron was split at 0.55b/2, and the outboard and inboard segments could be deflected individually or together.

The inboard aileron could also be deflected in combination with the inboard flap on the right wing to simulate 0.39b/2 trailing-edge flaps as can be seen in the photograph presented in figure 2.

Four strain-gage beams, two on each segment, connected the aileron to the wing. The aileron hinge moments and aileron normal forces were measured by resistance-type strain gages mounted on each of the four beams.

A flexible seal was installed between the wing and the aileron from 0.16b/2 to 0.95b/2. Four pressure orifices above and four below the aileron seal were installed at various spanwise stations in the basic wing just forward of each aileron segment and were connected by flexible tubing to a manometer board for the determination of pressure differences across the seal during the tests. The right wing was not equipped with a seal between the wing proper and the flap.

The photograph of the test setup (fig. 2) shows the three-support system employed during these tests.

Tests

The tests were made in the Langley 19-foot pressure tunnel with the air in the tunnel compressed to approximately $2\frac{1}{3}$ atmospheres. The

outboard 0.40b/2 aileron was deflected at various angles on both the plain wing and the wing having 0.79b/2 leading-edge flaps and 0.39b/2 trailing-edge flaps deflected. The 0.79b/2 aileron was deflected only on the plain-wing configuration.

The leading-edge flaps were deflected 30° in combination with the part-span trailing-edge flaps deflected 50°. The deflection angles were chosen to permit a comparison with data obtained from an unswept wing of aspect ratio 2.5 having the same wing area, taper ratio, and airfoil section as that of the subject wing. These flap deflections were also considered representative of the most favorable deflection angles tested for a wing of similar airfoil section and aspect ratio (ref. 1).

Measurements of moments and forces, aileron loads, hinge moments, and aileron balance-chamber pressure were made for each configuration through the angle-of-attack range from -4° to approximately 25° and for various aileron deflections from -25° to +25°. A dynamic pressure of 80 pounds per square foot, corresponding to a Reynolds number of 6.20×10^6 and a Mach number of 0.15, was maintained for most of the test conditions. Aileron hinge moments and normal forces exceeded the limits of the measuring instrument for a few maximum negative aileron deflection angles at low angles of attack and maximum positive aileron deflections at high angles of attack; therefore, for these angles the dynamic pressure was lowered to 60 pounds per square foot, which corresponded to a Reynolds number of 5.36×10^6 and a Mach number of 0.13. This small Reynolds number change had no apparent effect on the trends and magnitudes of the data presented.

CORRECTIONS TO DATA

The lift and pitching-moment coefficients (fig. 3) have been corrected for air-stream misalinement and for support tare and interference effects. The dynamic pressure has been corrected for blockage in the test section. Jet-boundary corrections, based on the method of reference 2, have been applied to the angle of attack but were found to be negligible for the pitching-moment coefficient, yawing-moment coefficient, and rolling-moment coefficient and were not applied.

Variations of rolling-moment and yawing-moment coefficients at $\delta_a = 0°$ through the angle-of-attack range were obtained for both the plain wing and the wing with leading- and trailing-edge flaps deflected. A check run, made for the plain-wing configuration, showed little change in the magnitude of moment-coefficient variations (fig. 4). The moment coefficient of both plain-wing runs at $\delta_a = 0°$ were averaged and applied as tares to the rolling-moment and yawing-moment data. Similarly, the yawing- and rolling-moment coefficients of the leading- and trailing-edge flap configurations at $\delta_a = 0°$ were applied as tares to the

flapped configuration data. The moment coefficients indicated at $\delta_a = 0^\circ$ are due to air-stream misalinement across the tunnel test section and possible slight model asymmetry.

A calibration of the aileron-seal leakage before the tests were made indicated that average ratios K of pressure differences across the seal were 0.871 and 0.844 of the pressure differences across the vents for the full-span and the outboard aileron, respectively. The same seal was used for all tests and the two conversion factors K were used to convert the pressure differences across the seal to pressure differences across the vents in order to approximate a balance chamber with a perfect seal. The seal leakage was attributed to the discontinuity of the seal along the aileron span at the strain-gage beam position and the openings around the ends of the 0.79b/2 aileron and at the split section dividing the two aileron segments.

After the tests had been completed, another seal calibration indicated K values to be less than 3 percent lower than on the previous calibration for both the 0.79b/2 and the outboard 0.40b/2 aileron. This percentage is considered to be within the accuracy of the calibration and it has been determined that the small differences in seal calibrations had a negligible effect on the P_R values corrected to a perfect sealed condition.

RESULTS

The basic aileron data are presented in figures 5 to 7 and the results have been summarized in figure 8. The outboard aileron effectiveness C_{l_δ} of the plain wing at an angle of attack of 0° was calculated to be 0.00132 from the method of reference 3 as compared with the experimental value of 0.00150. The addition of leading- and trailing-edge flaps decreased the experimental C_{l_δ} slightly in the angle-of-attack range below 6° and increased C_{l_δ} for angles of attack greater than 6° (fig. 8). The aileron effectiveness of the plain wing was increased substantially by the use of the 0.79b/2 aileron at all angles of attack for which C_{l_δ} was measured. The aileron effectiveness of the outboard aileron with leading- and trailing-edge flaps deflected, however, was greater beyond an angle of attack of approximately 12° than that of the plain wing with either 0.79b/2 aileron or outboard 0.40b/2 aileron.

A comparison of aileron effectiveness values for the unswept wing of aspect ratio 4.0 with an unswept wing of aspect ratio 2.5 having the same wing area, taper ratio, and airfoil section is presented in figure 9.

As expected, the aileron effectiveness of the aspect ratio 4.0 wing is greater than that of the aspect ratio 2.5 wing through most of the linear lift range for all three test configurations.

Comparisons of C_{h_α} and C_{h_δ} values of both wings are presented in figures 10 and 11.

Langley Aeronautical Laboratory,
National Advisory Committee for Aeronautics,
Langley Field, Va.

REFERENCES

1. Johnson, Ben H., Jr., and Bandettini, Angelo: Investigation of a Thin Wing of Aspect Ratio 4 in the Ames 12-Foot Pressure Wind Tunnel. II - The Effect of Constant-Chord Leading- and Trailing-Edge Flaps on the Low-Speed Characteristics of the Wing. NACA RM A8F15, 1948.

2. Sivells, James C., and Salmi, Rachel M.: Jet-Boundary Corrections for Complete and Semispan Swept Wings in Closed Circular Wind Tunnels. NACA TN 2454, 1951.

3. DeYoung, John: Theoretical Antisymmetric Span Loading for Wings of Arbitrary Plan Form at Subsonic Speeds. NACA Rep. 1056, 1951. (Supersedes NACA TN 2140.).

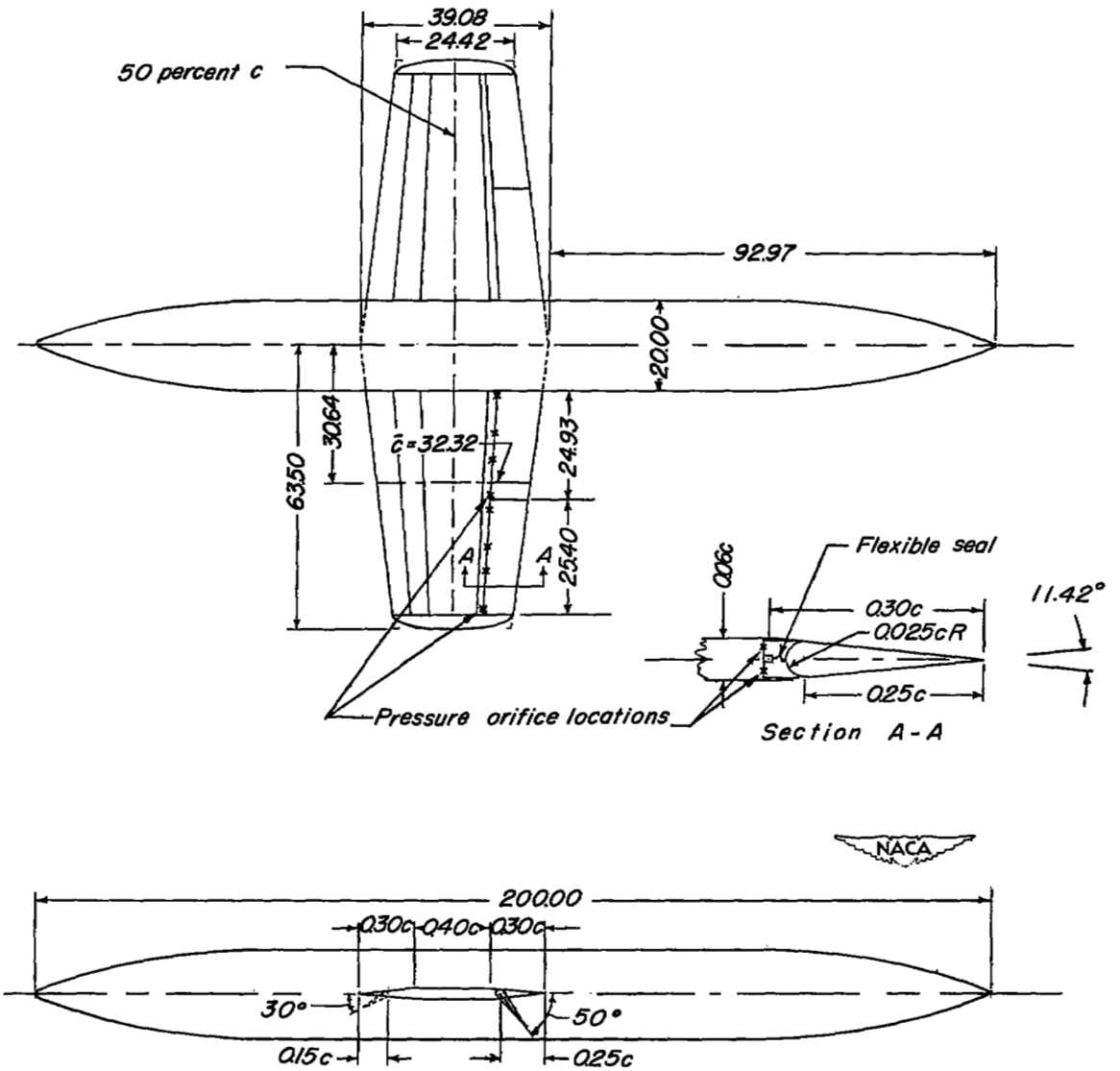

Figure 1.- Geometry of the model and aileron details. All dimensions are in inches unless otherwise noted. A, 4.0; S, 28 square feet; λ, 0.625.

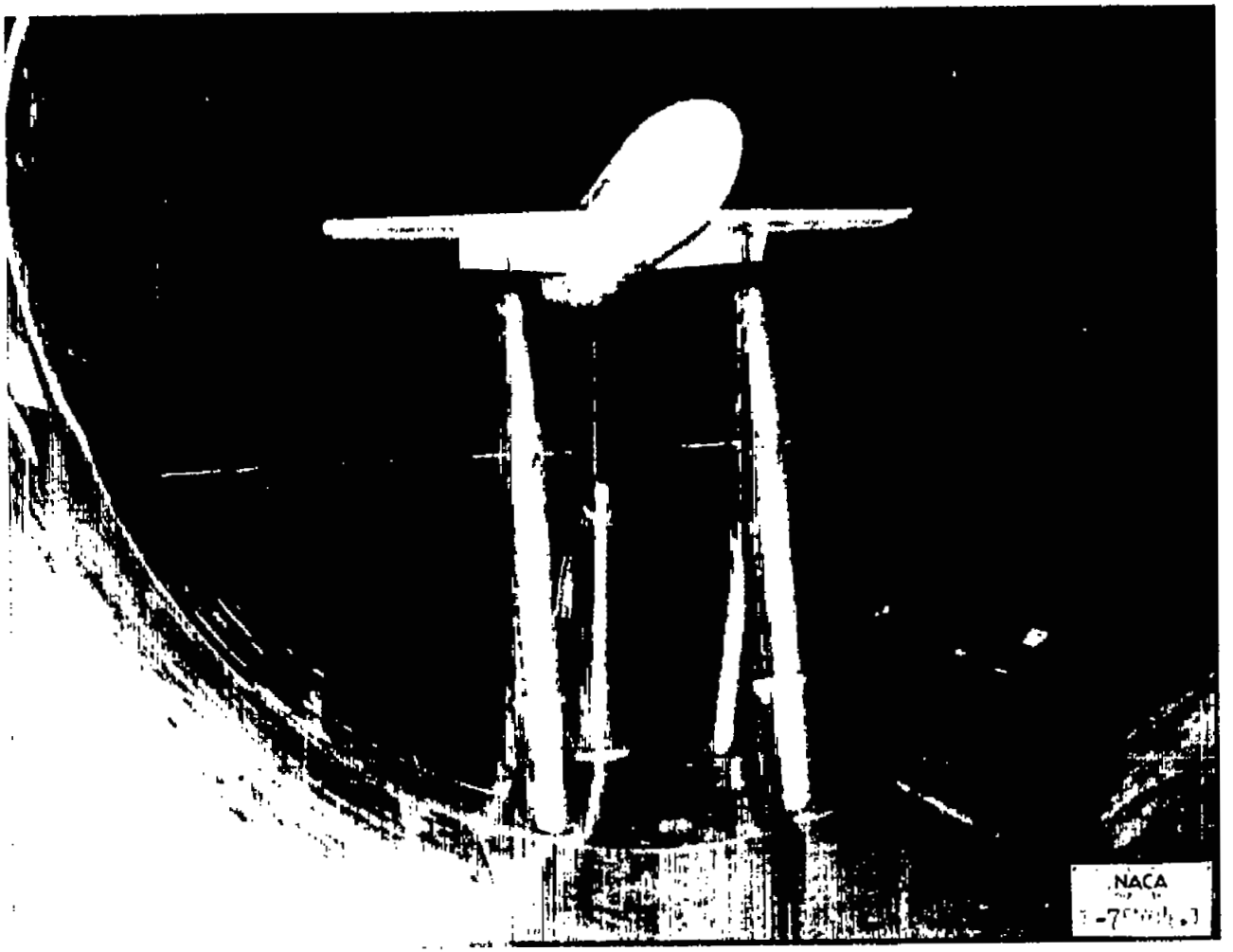

Figure 2.- Model mounted on three-support system in the Langley 19-foot pressure tunnel with full-span leading-edge flaps and part-span trailing-edge flaps deflected. Front view.

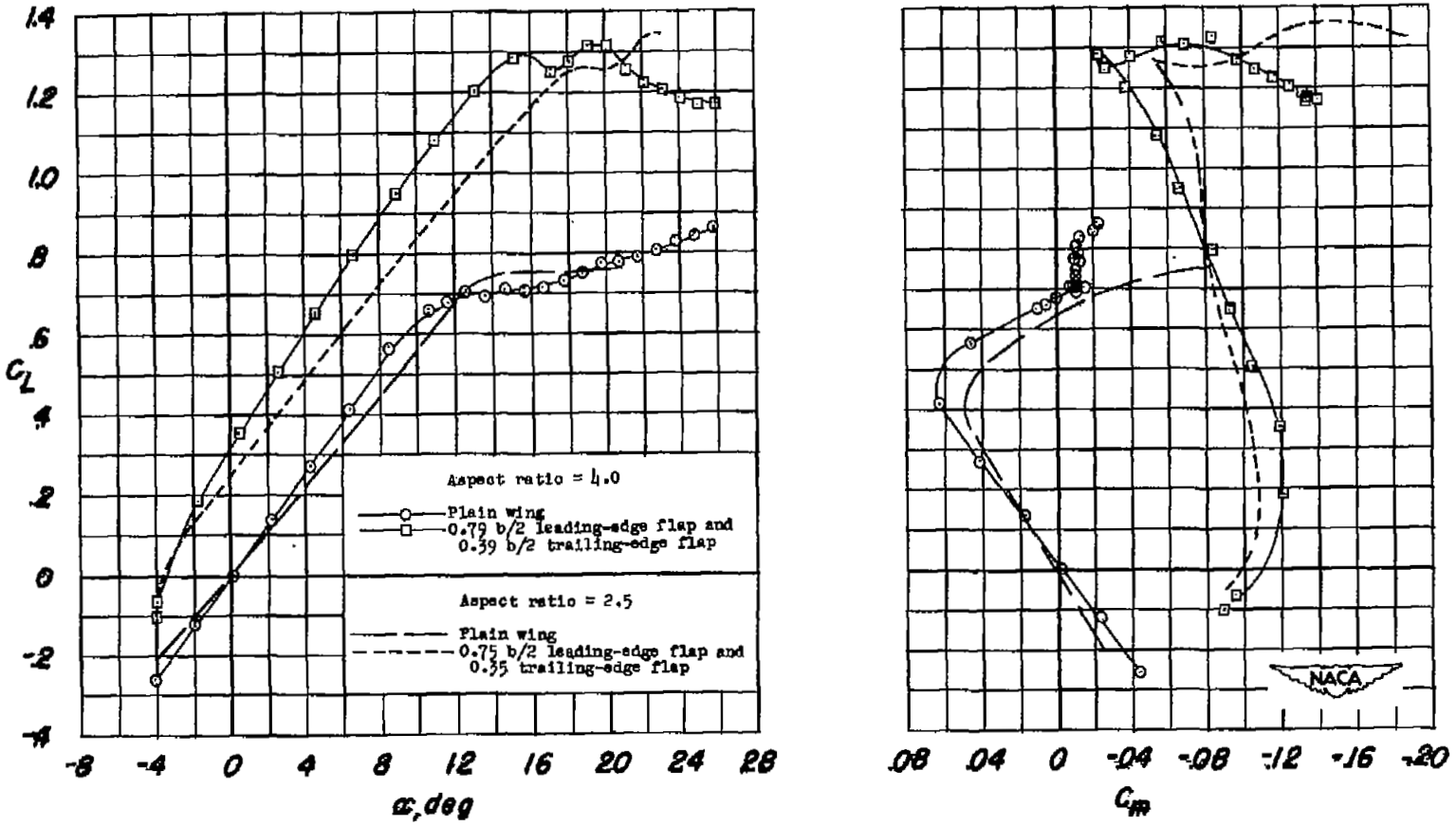

Figure 3.- Comparisons of lift and pitching-moment coefficient of the subject aspect ratio 4.0 wing with that of a wing of aspect ratio 2.5 having the same wing area, taper ratio, and airfoil section. $\delta_f = 50^\circ$; $\delta_n = 30^\circ$.

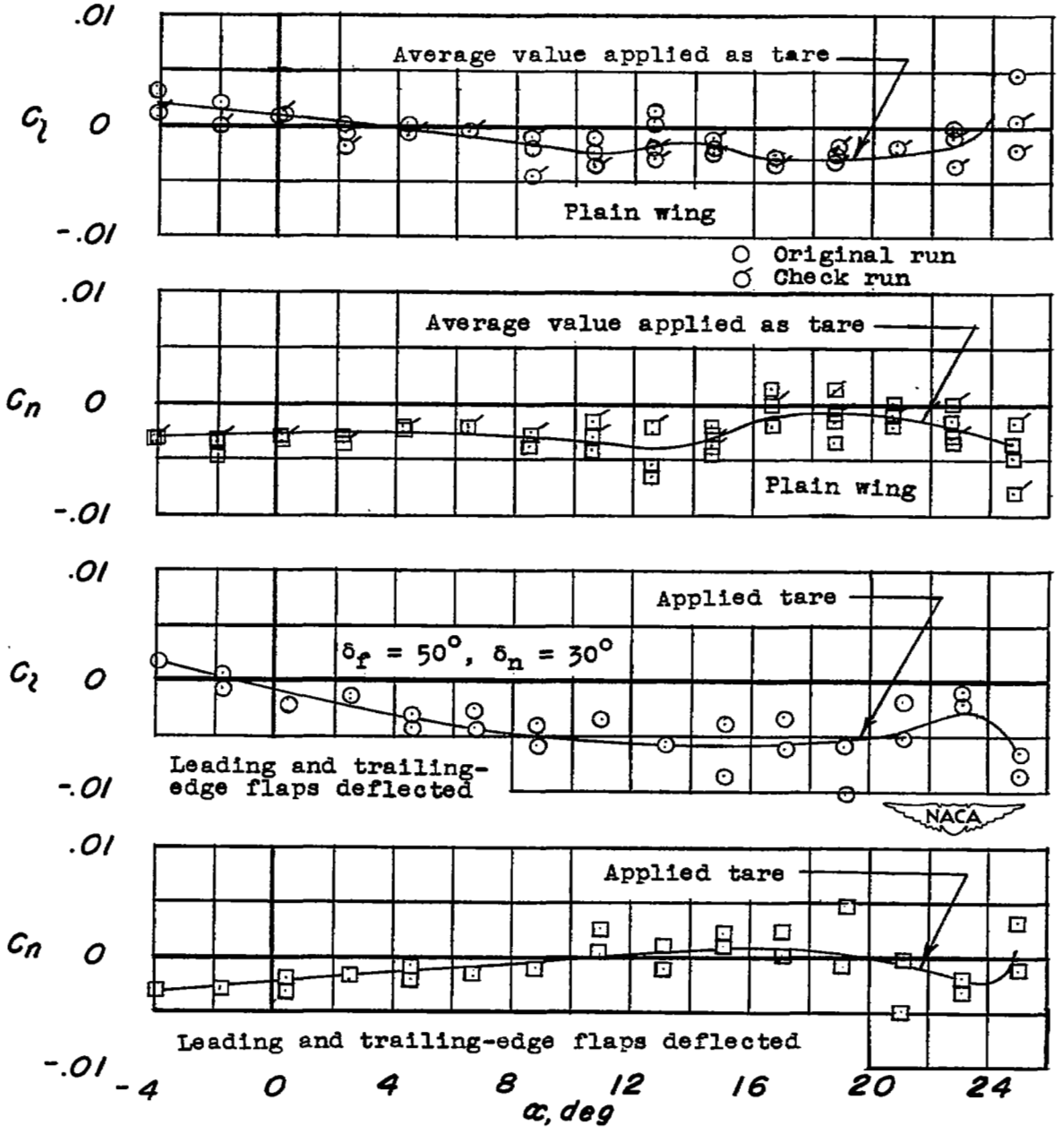

Figure 4.- Static rolling-moment and yawing-moment coefficients with and without leading- and trailing-edge flaps deflected and the tares applied to the data. $\delta_a = 0°$.

[redacted]

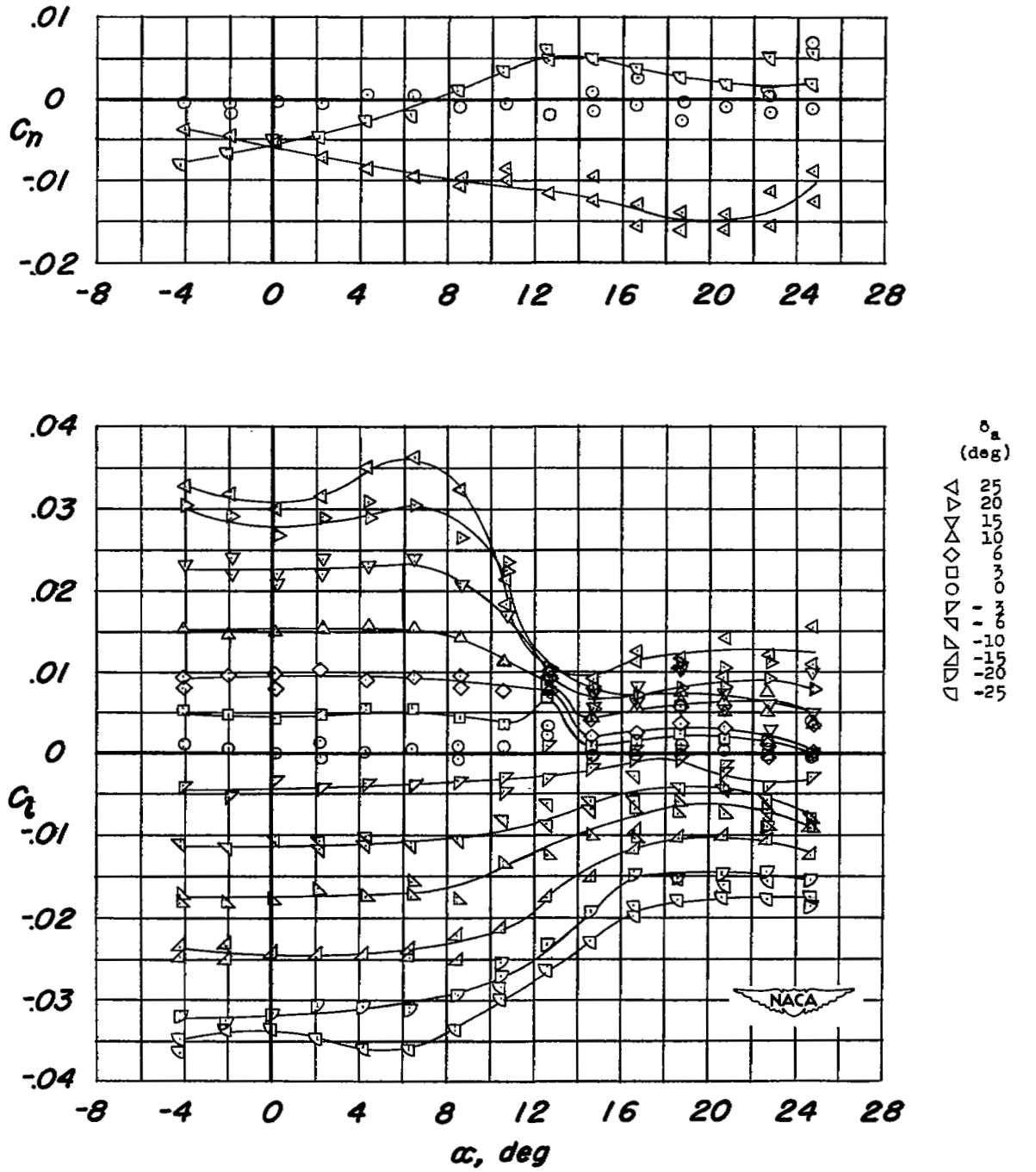

(a) Variation of C_n and C_l with α.

Figure 5.- Variation of C_n, C_l, C_{h_a}, P_R, and C_{N_a} with α; 0.40b/2 outboard aileron. Plain wing.

[redacted]

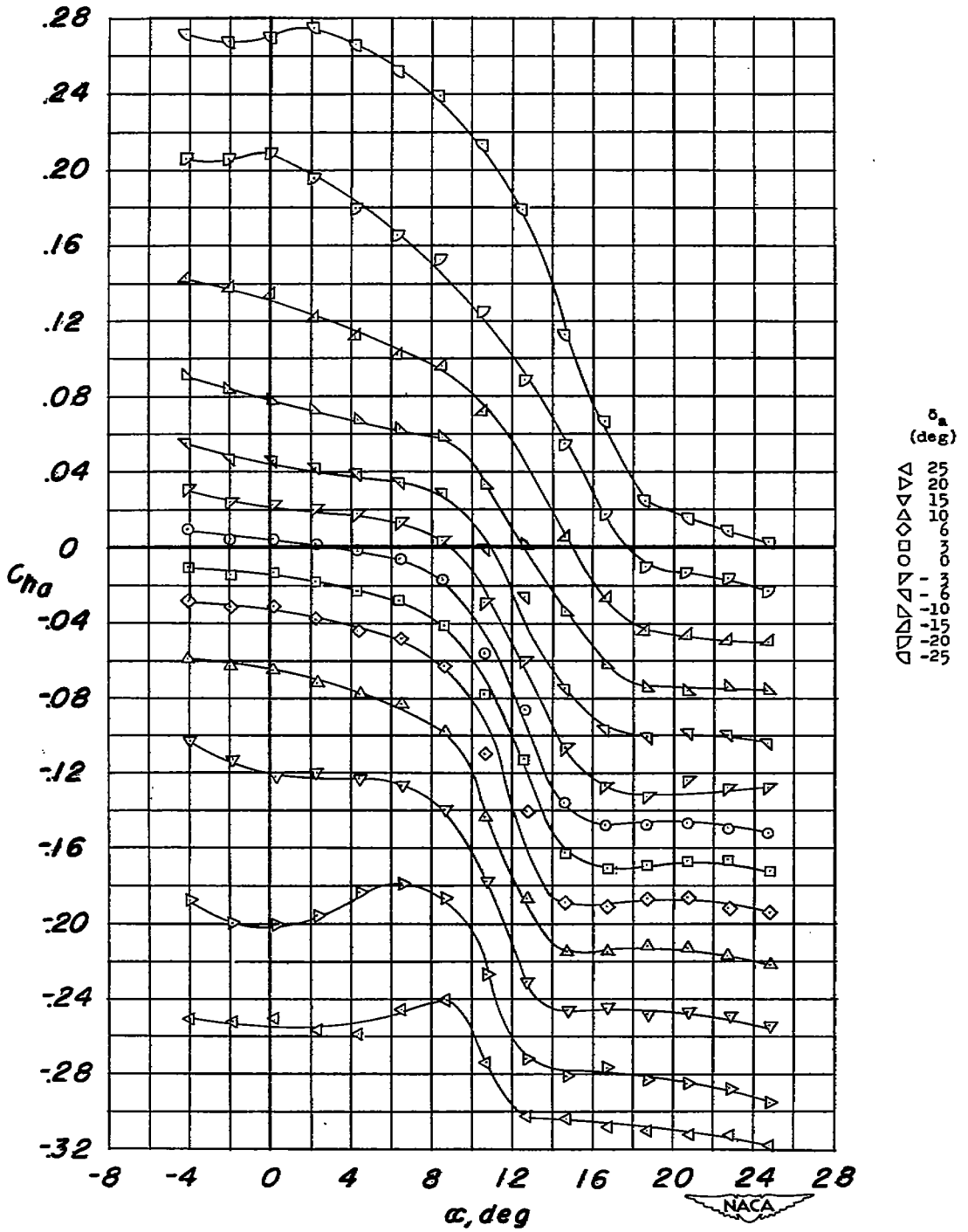

(b) Variation of C_{h_a} with α.

Figure 5.- Continued.

[redacted]

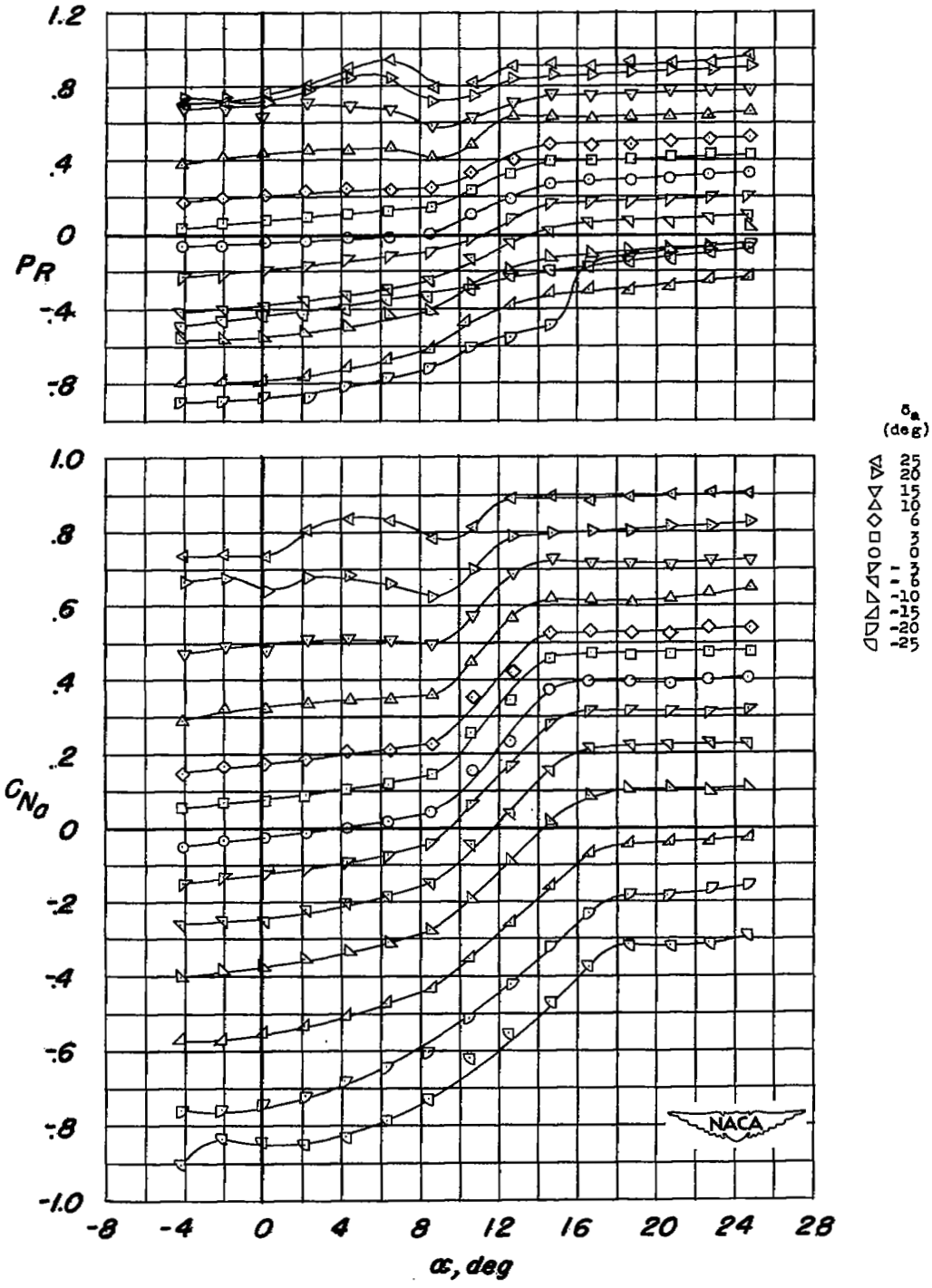

(c) Variation of P_R and C_{N_a} with α.

Figure 5.- Concluded.

[redacted]

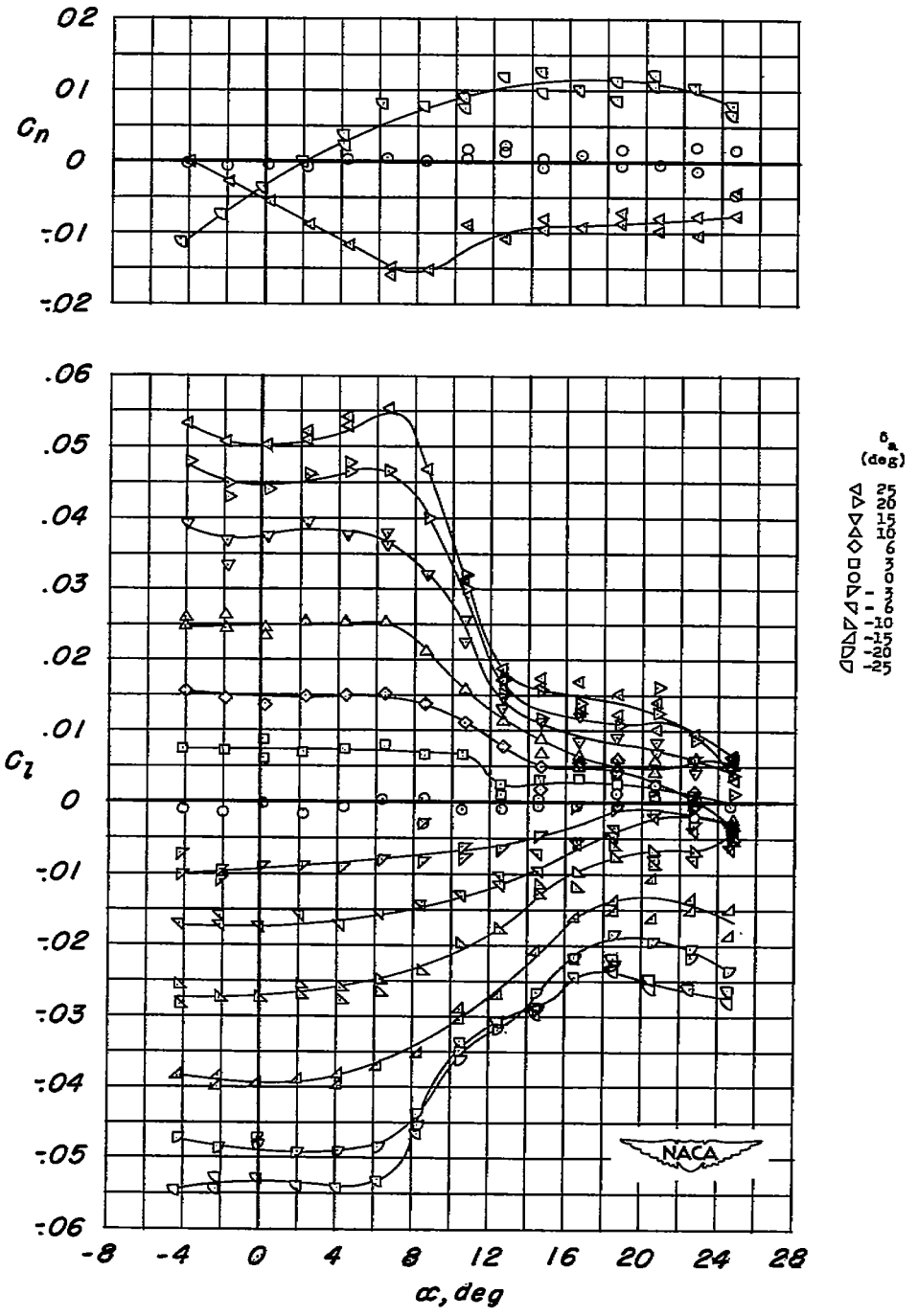

(a) Variation of C_n and C_l with α.

Figure 6.- Variation of C_n, C_l, C_{h_a}, P_R, and C_{N_a} with α; 0.79b/2 aileron. Plain wing.

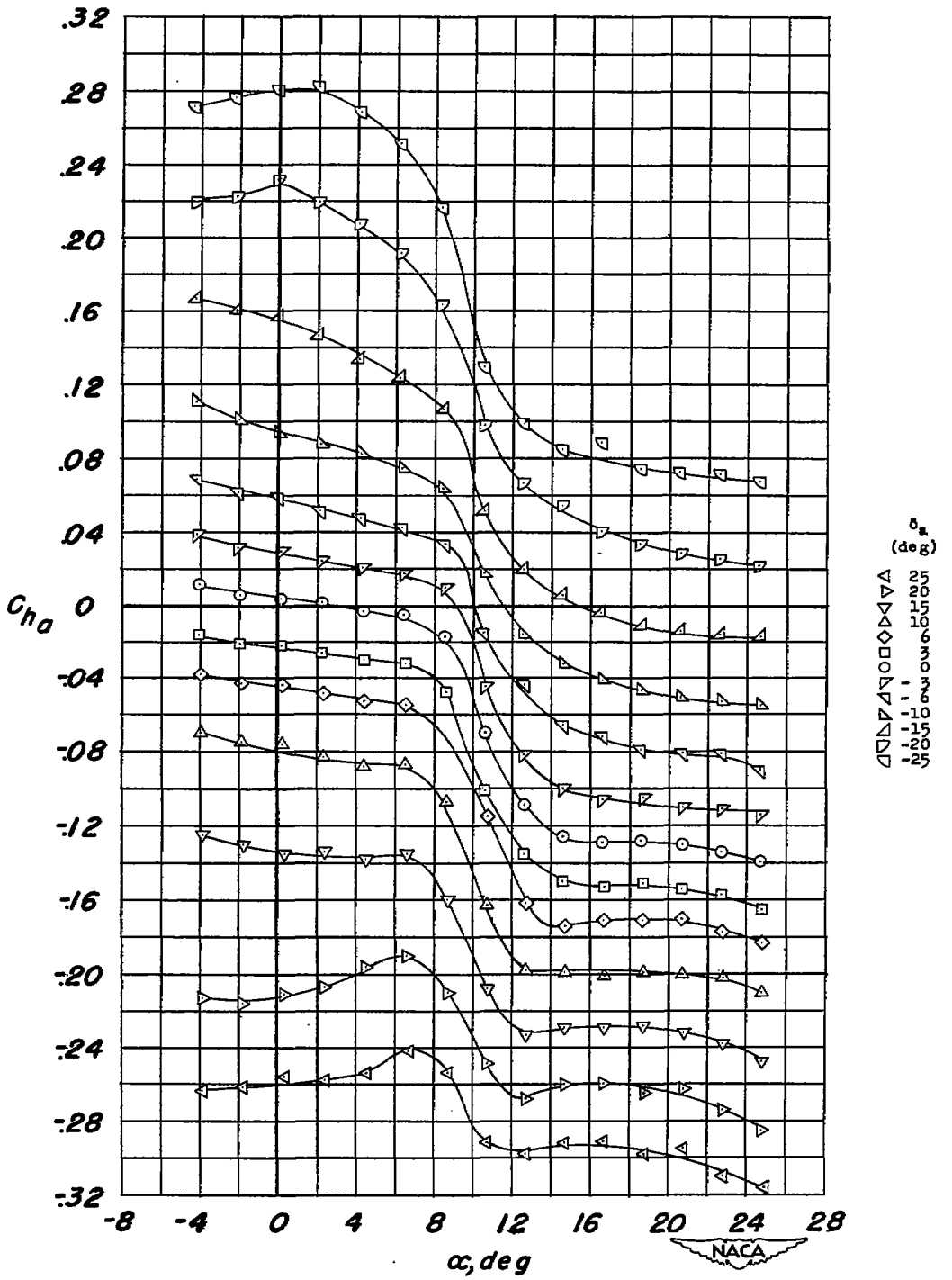

(b) Variation of C_{h_a} with α.

Figure 6.- Continued.

[redacted]

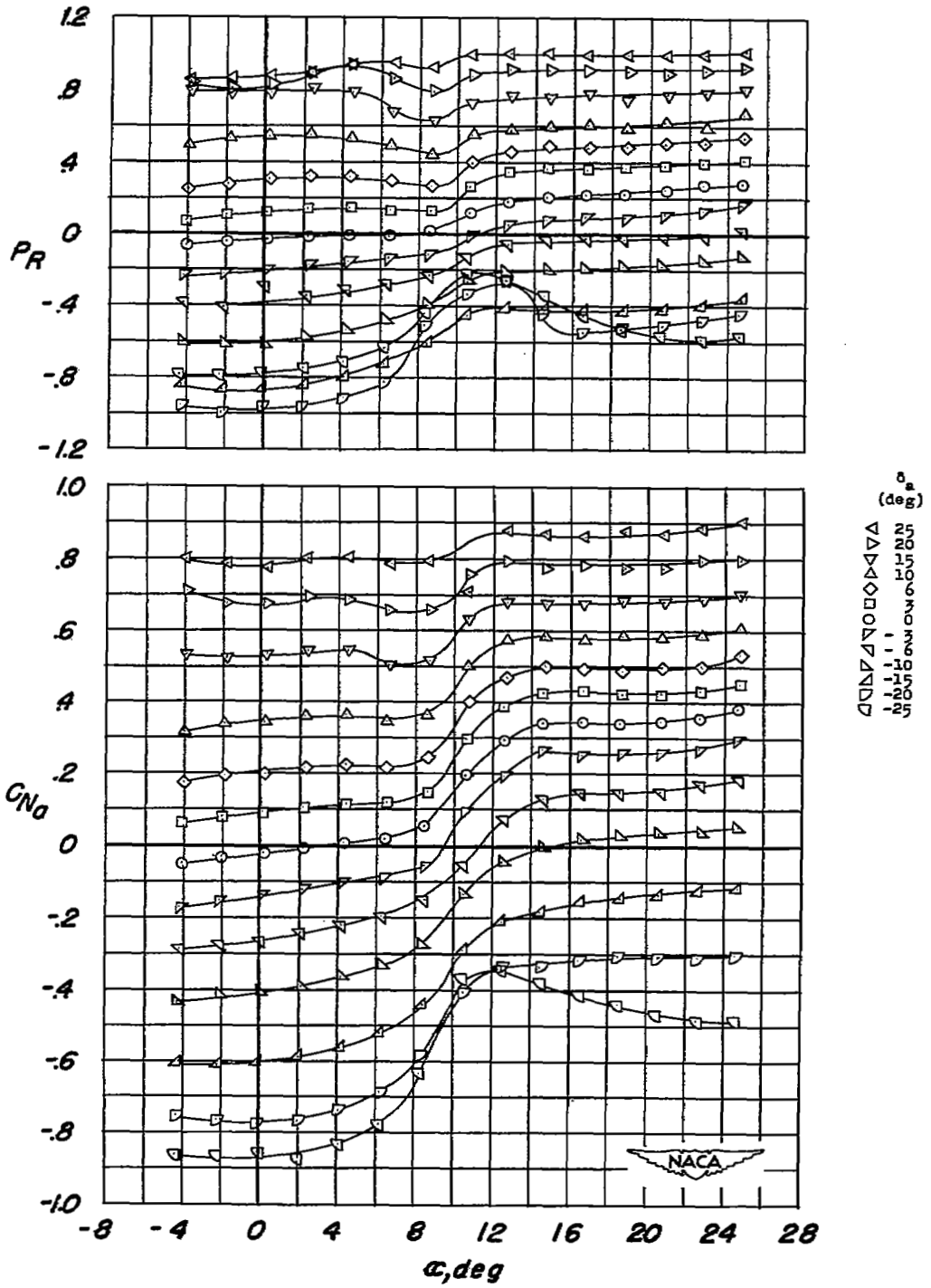

(c) Variation of P_R and C_{N_a} with α.

Figure 6.- Concluded.

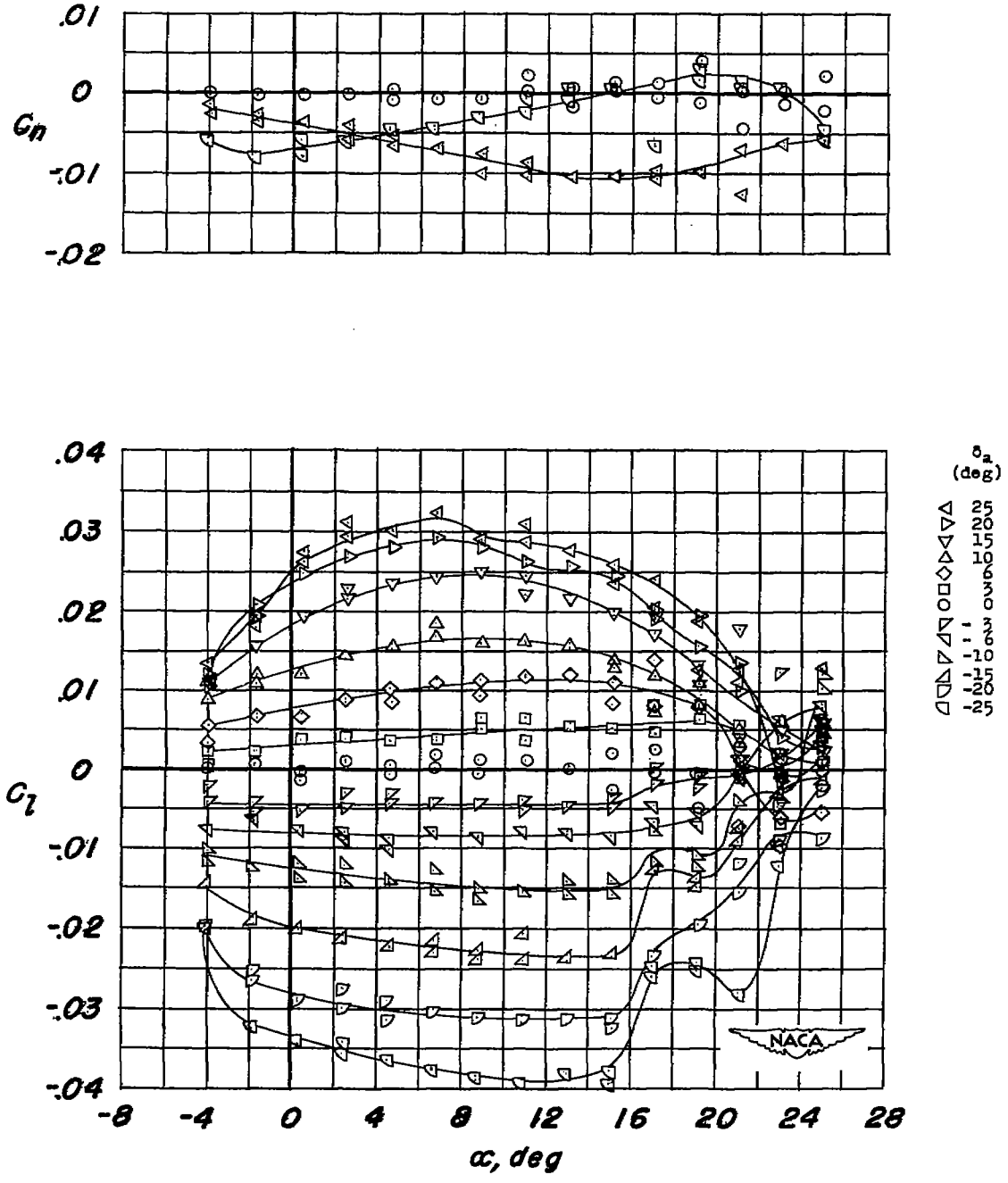

(a) Variation of C_n and C_l with α.

Figure 7.- Variation of C_n, C_l, C_{h_a}, P_R, and C_{N_a} with angle of attack; 0.79b/2 leading-edge flaps, 0.39b/2 trailing-edge flaps, 0.40b/2 outboard aileron. $\delta_f = 50^\circ$; $\delta_n = 30^\circ$.

[redacted]

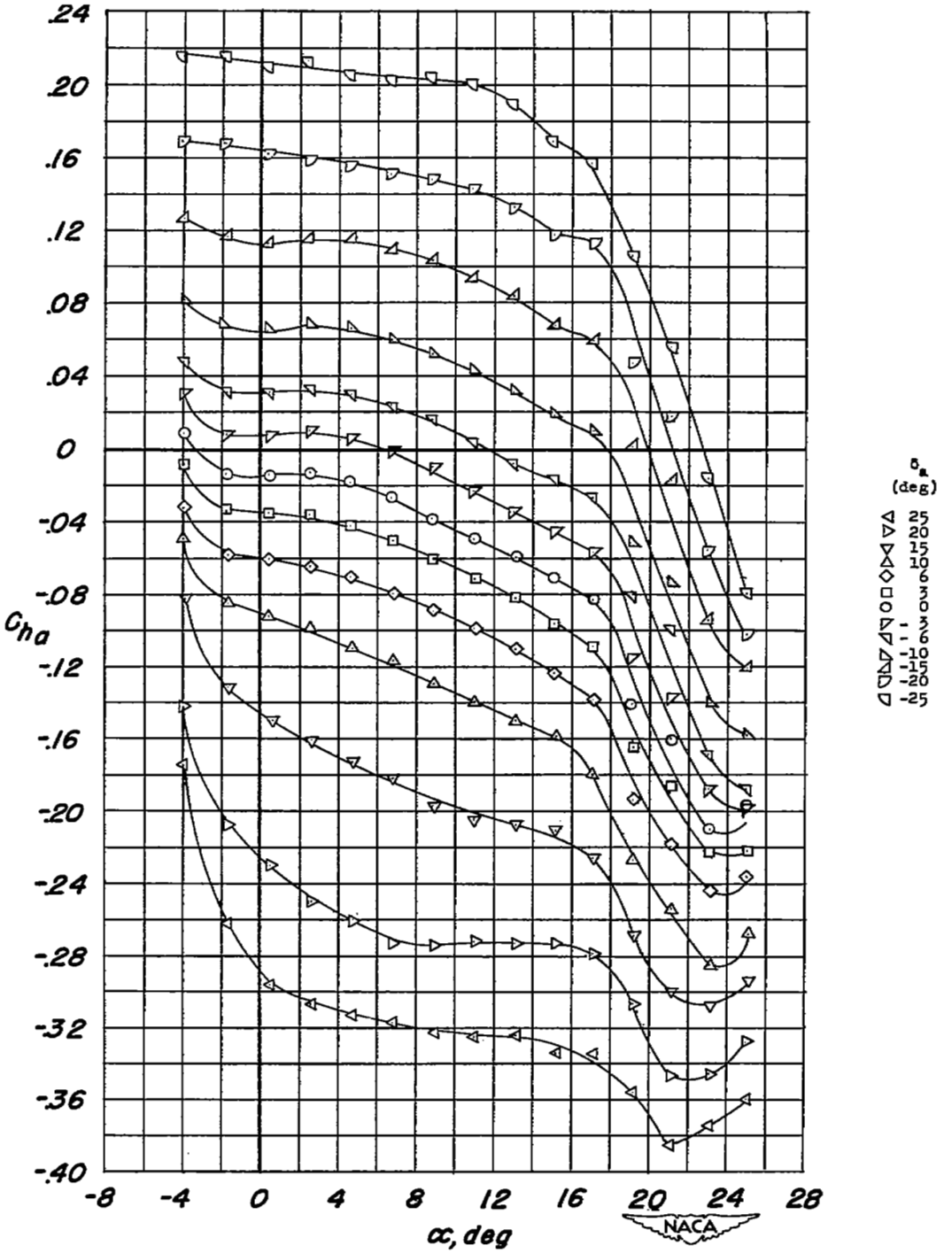

(b) Variation of C_{h_a} with α.

Figure 7.- Continued.

[redacted]

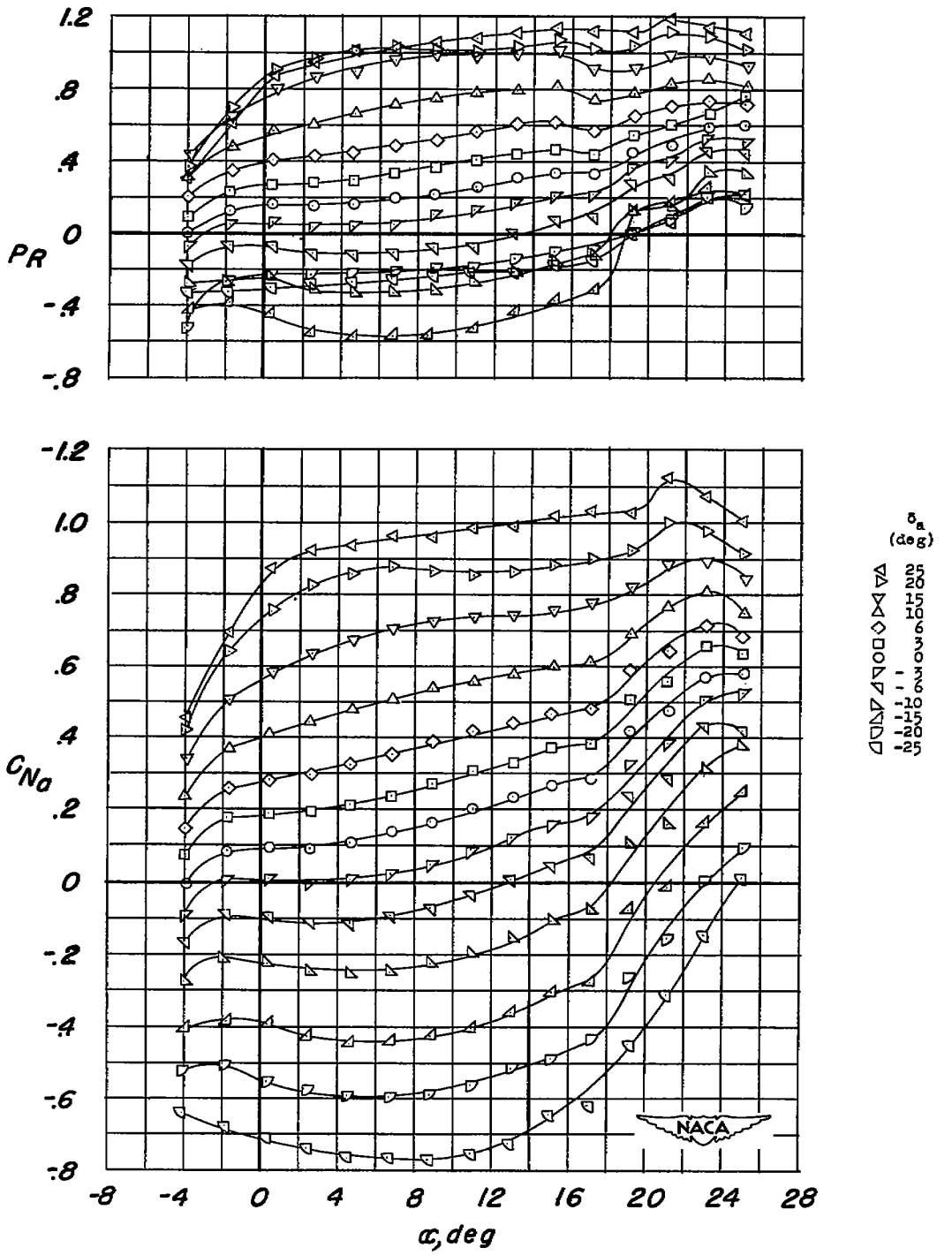

(c) Variation of P_R and C_{N_a} with α.

Figure 7.- Concluded.

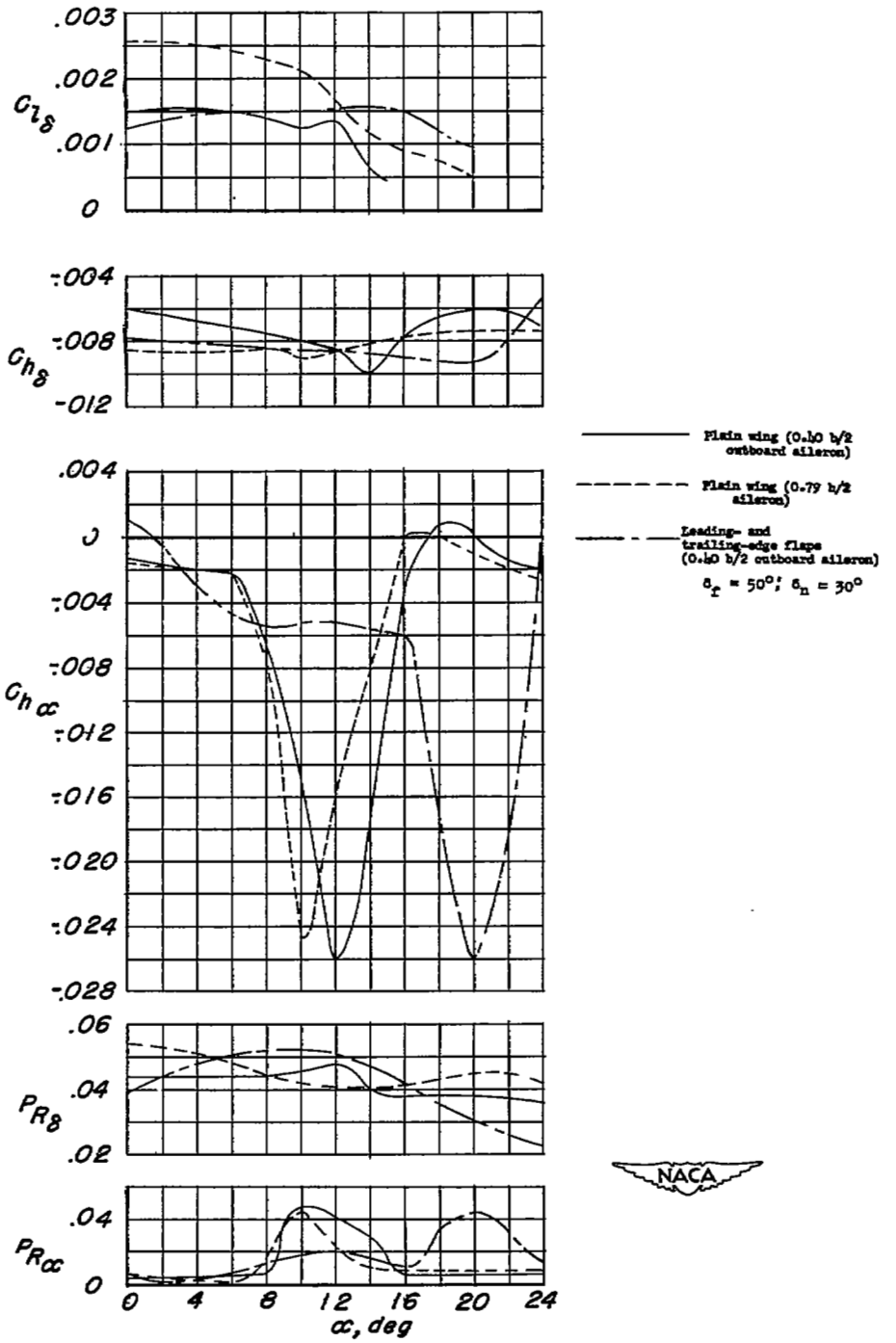

Figure 8.- The effects of aileron span and leading- and trailing-edge flaps on the aileron hinge moment and effectiveness paramters C_{l_δ}, C_{h_δ}, C_{h_α}, P_{R_δ}, P_{R_α}.

[redacted]

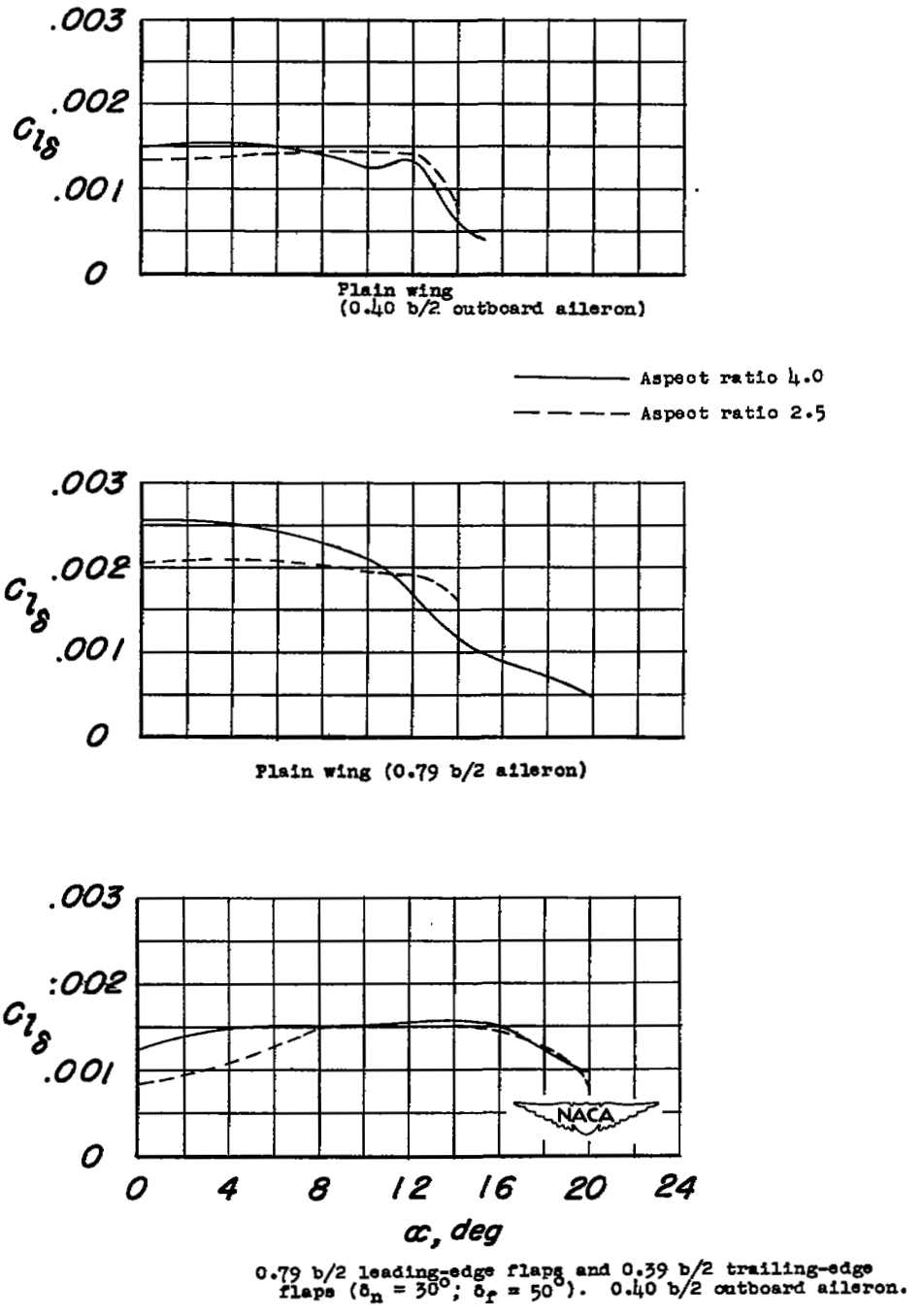

Figure 9.- Comparison of aileron effectiveness C_{l_δ} of the subject aspect ratio 4.0 wing with that of a wing of aspect ratio 2.5 having the same area, taper ratio, and airfoil section.

[redacted]

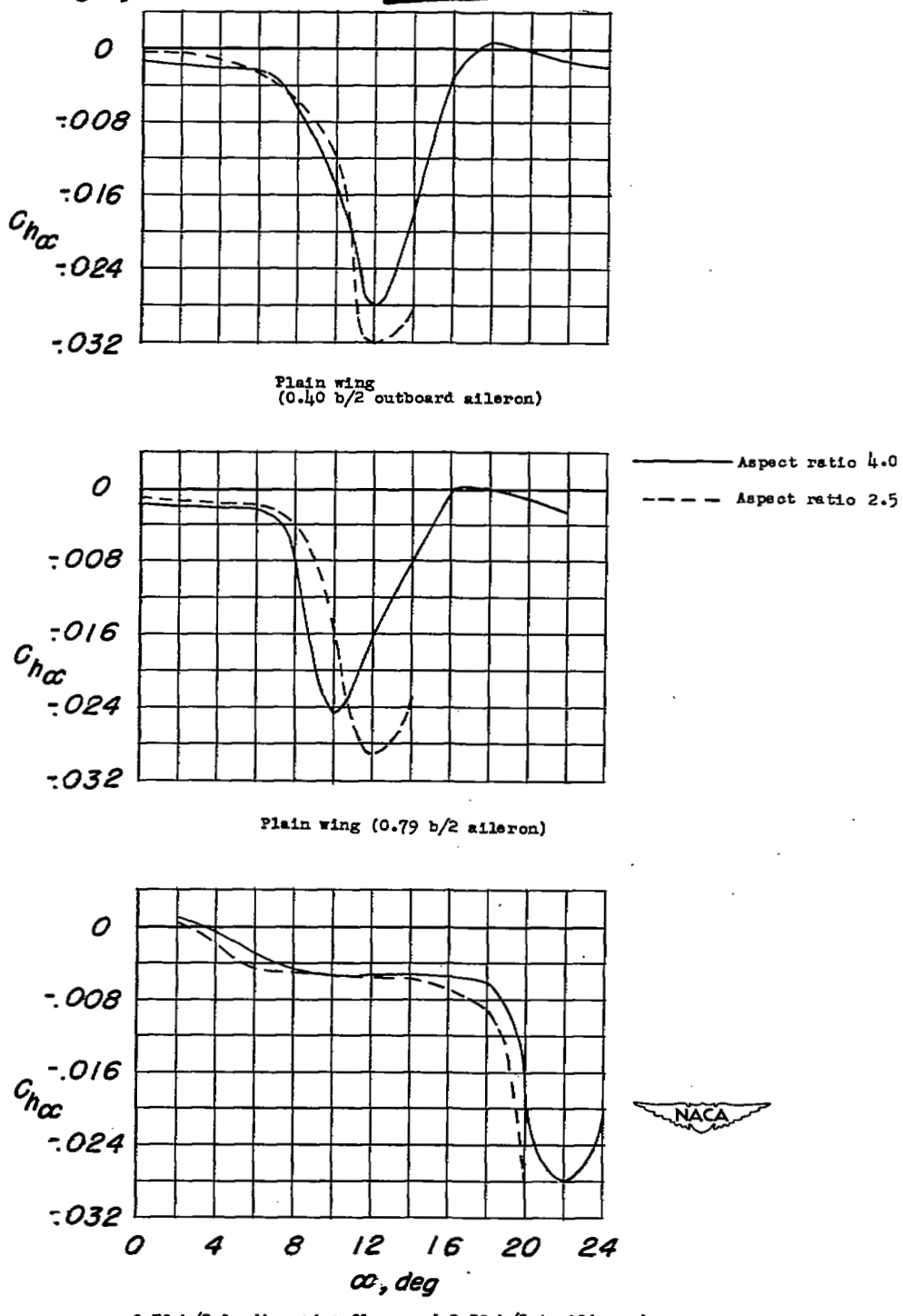

Figure 10.- Comparison of C_{h_α} of the subject aspect ratio 4.0 wing with that of a wing of aspect ratio 2.5 having the same area, taper ratio, and airfoil section.

[redacted]

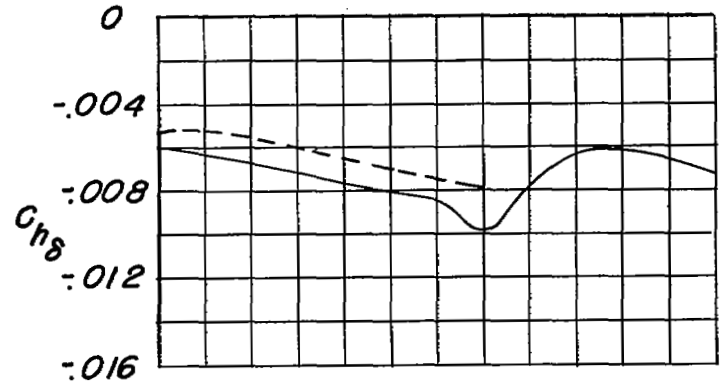

Plain wing
(0.40 b/2 outboard aileron)

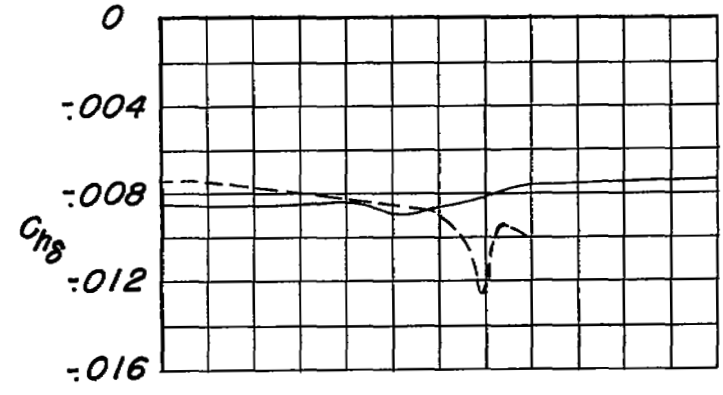

Plain wing (0.79 b/2 aileron)

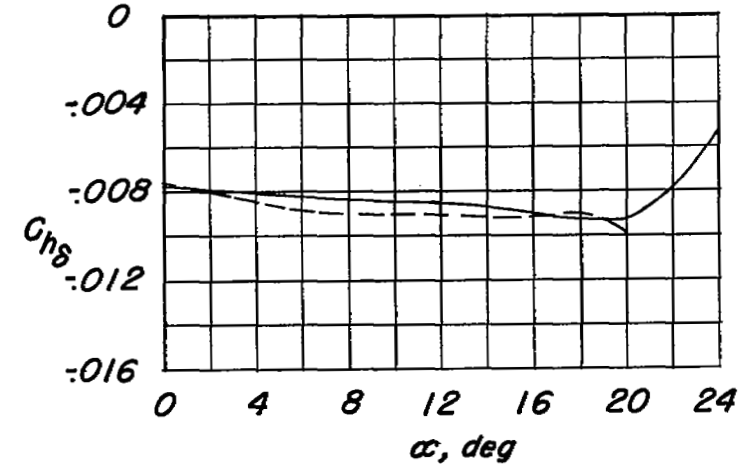

0.79 b/2 leading-edge flaps and 0.39 b/2 trailing-edge flaps ($\delta_n = 30°$, $\delta_f = 50°$). 0.40 b/2 outboard aileron.

——— Aspect ratio 4.0

– – – – Aspect ratio 2.5

Figure 11.- Comparison of C_{h_δ} of the subject aspect ratio 4.0 wing with that of a wing of aspect ratio 2.5 having the same area, taper ratio, and airfoil section.

NACA-Langley - 3-20-53 - 325